Deletion of CFTR Translation Start Site Reveals Functional Isoforms of the Protein in CF Patients

Anabela S. Ramalho[1,2], Marzena A. Lewandowska[3], Carlos M. Farinha[1,2], Filipa Mendes[†1,2], Juan Gonçalves[4], Celeste Barreto[5], Ann Harris[3] and Margarida D. Amaral[1,2]

[1]University of Lisboa, Faculty of Sciences, Centre for Biodiversity, Functional and Integrative Genomics (BioFIG), Lisboa, Portugal, [2]Department of Genetics, National Institute of Health, Lisboa, Portugal, [3]Human Molecular Genetics Program, Children's Memorial Research Center, Northwestern University, Chicago IL, USA, [4]Hospital do Divino Espírito Santo, Ponta Delgada, Portugal, [5]Hospital de Santa Maria, Lisboa, Portugal, [†]Current Address: Chemical and Radiopharmaceutical Sciences Unit, Nuclear and Technological Institute, Sacavém, Portugal

Abstract
Background/Aims: Mutations in the *CFTR* gene cause Cystic Fibrosis (CF) the most common life-threatening autosomal recessive disease affecting Caucasians. We identified a CFTR mutation (c.120del23) abolishing the normal translation initiation codon, which occurs in two Portuguese CF patients. This study aims at functionally characterizing the effect of this novel mutation. Methods: RNA and protein techniques were applied to both native tissues from CF patients and recombinant cells expressing CFTR constructs to determine whether c.120del23 allows CFTR protein production through usage of alternative internal codons, and to characterize the putative truncated CFTR form(s). Results: Our data show that two shorter forms of CFTR protein are produced when the initiation translation codon is deleted indicating usage of internal initiation codons. The N-truncated CFTR generated by this mutation has decreased stability, very low processing efficiency, and drastically reduced function. Analysis of mutants of four methio- nine codons downstream to M1 (M82, M150, M152, M156) revealed that each of the codons M150/M152/ M156 (exon 4) can mediate CFTR alternative translation. Conclusions: The CFTR N-terminus has an important role in avoiding CFTR turnover and in rendering effective its plasma membrane traffic. These data correlate well with the severe clinical phenotype of CF patients bearing the c.120del23 mutation.

Introduction

Mutations in the Cystic Fibrosis Transmembrane Conductance Regulator (*CFTR*, MIM# 602421) gene cause Cystic Fibrosis (CF, MIM# 219700) the most common life-threatening autosomal recessive disease among Caucasians [1]. The major CF symptoms are progressive pulmonary dysfunction, pancreatic insufficiency and elevated sweat electrolyte concentration [1]. CFTR protein, a Cl⁻ channel in the apical membrane of epithelial cells comprises several domains, namely: two membrane-

spanning domains (MSD1/2), two nucleotide binding domains (NBD1/2) and a regulatory domain (RD), besides the N- and C-termini which are both also functionally relevant [2, 3].

Although ~1,600 variants of the *CFTR* gene have been identified [4], F508del, the most frequent mutation (~70% of CF chromosomes worldwide) is associated with a severe clinical phenotype. Most F508del-CFTR is retained and degraded at the level of the endoplasmic reticulum (ER) [5]. In Southern Europe the incidence of F508del is lower, in Portugal it only accounts for ~60% of CF chromosomes [6]. Hence, there is a higher prevalence of non-F508del alleles among Portuguese CF patients and this necessitates close assessment of other predicted mutations to determine their functional consequences at the cellular and physiological levels. The functional characterization of such naturally occurring CFTR mutations is of high relevance for genetic counselling and clinical prognosis, not just for such gene variants, but also for mutations in other disease-associated genes which perturb the same molecular mechanism.

Here, we describe a novel CFTR mutation in exon 1, c.120del23, which we reported previously [4], that was found in two CF patients from the Azores islands, both with F508del in the other allele. As deletion of these 23 nucleotides (120-142) removes the translation initiation codon (133-135), we asked whether this mutation still allows for synthesis of CFTR protein through usage of alternative internal initiation codon(s), as shown for other CFTR variants [7]. We demonstrate that truncated CFTR proteins are produced and show that M150/M152/M156 (but not M82) can mediate this alternative translation initiation. By functionally characterizing these N-truncated protein(s) we show that at least one of these reaches the cell membrane, but it is unstable and has drastically reduced Cl- channel activity. These findings correlate well with the severe clinical phenotype of the two patients bearing this mutation.

Materials and Methods

DNA analysis
The 27 CFTR exons, intronic flanking regions, 5' and 3' UTRs and $[TG]_m T_n$ were analysed by sequencing as described elsewhere [8].

Transcript analysis
Following approval of this study by the hospital ethical committee and written informed consent from the parents, nasal epithelial cells from one of the CF patients with the F508del/ c.120del23 genotype were obtained. RNA extraction and cDNA synthesis were performed as described before [9]. Briefly, quantitative (log-phase) RT-PCR analysis of CFTR transcripts from nasal epithelial cells was performed in the region of exons 8-10, using a FAM-labelled primer [10]. After separation in the automatic sequencer, quantitative analysis of RT-PCR products was performed with the GeneScan® software as before [10].

In silico analysis of the potential alternative in-frame initiation codons
The CFTR mRNA sequence (GenBank:M28668, position 1-4575) was assessed for in-frame AUG codons as possible alternative initiation codons using the "AUG evaluator" and Open-Reading-Frame-Finder online software [11].

Constructs
By site-directed mutagenesis (QuikChange, Stratagene, La Jolla, CA, USA) c.120del23 was introduced into the wt-CFTR-cDNA in the pNUT mammalian expression vector [12, 13] using as primer the patient's RT-PCR product (positions 96-265). The exon-1-lacking-CFTR-cDNA-construct for *in vitro* translation resulted from cloning (CFTR-cDNA, exons 2-24) into the pSP73 vector. Other CFTR mutants were produced by mutagenesis on c.120del23-CFTR-cDNA-pNUT or on the exon2-24-CFTR-cDNA-pSP73 (primers shown in Table 1).

Stable CFTR-expressing BHK cells
The c.120del23-CFTR cDNA pNUT plasmid and its methionine mutants were used (2 μg) to produce novel stable baby hamster kidney (BHK) cell lines by transfection with lipofectin (Invitrogen, Paisley, UK) according to the manufacturer's instructions. The novel cell lines stably expressing these constructs were cultivated under metothrexate (500 μM) selection as previously described [14, 15].

Biochemical analysis
CFTR protein expression assessment by Western blot (WB) was performed as described [16] using the anti-CFTR monoclonal antibody (Ab) M3A7 (Millipore, Hampshire, UK) and the SuperSignal® West Pico chemiluminescent substrate system (Thermo Scientific, Rockford, IL, USA). Metabolic pulse-labelling of cells, CFTR immunoprecipitation (IP), electrophoresis, fluorography, and densitometry were also performed as described before [17].

Immunocytochemistry
Immunofluorescence was also performed as previously [18]. Briefly, CFTR-transfected BHK cells grown on chamberslides (Nalgene Nunc, Roskilde, Denmark) were fixed in methanol, permeabilized and incubated for 1h with 24-1 monoclonal anti-CFTR antibody (R&D Systems, Minneapolis, MN, USA) and after washing, incubated with FITC-secondary antibody (Amersham Biosciences Corp, Piscataway, NJ, USA) and mounted in Vectashield (Sigma-Aldrich Corp, St. Louis, MO, USA) with DAPI (blue) for nuclear staining. Preparations were observed in a Zeiss Axioskop fluorescence microscope and microphotographs obtained with a Photometrics image point cooled CCD video camera.

Ramalho/Lewandowska/Farinha/Mendes/Gonçalves/Barreto/Harris/ Amaral

Table 1. Primers used for site-directed mutagenesis. Primers used to mutagenize the CFTR methionines in positions 82, 150, 152 and 156 into valines in the 120del23-CFTR-pNUT and in the pSP73CFTRex2-24 constructs.

Construct	Primers (name: sequence 5'-> 3')
pNUT 120del23-CFTR	M82V.F: CGATGTTTTTTCTGGAGATT TGTGTTCTATGGAATC
	M82V.R: GATTCCATAGAACACAAAT CTCCAGAAAAAACATCG
	M150V: CCTTCATCACATTGGAGTGC AGATGAGAATAG
	M150V R: CTATTCTCATCTGCACTCC AATGTGATGAAGG
	M152V.F: CATTGGAATGCAGGTGAGAA TAGCTATG
	M152V.R: CATAGCTATTCTCACCTGC ATTCCAATG
	M156V.F: GATGAGAATAGCTGTGTTTA GTTTG
	M156V.R: CAAACTAAACACAGCTATT CTCATC
	M150V/M152V.F: CTTCATCACATTGGAGTGCA GGTGAGAATAGCTATGTTTA GTTTG
	M150V/M152V R: CAAACTAAACATAGCTATT CTCACCTGCACTCCAATGTG ATGAAG
	M150V/M156V.F: CTTCATCACATTGGAGTGCA GATGAGAATAGCTGTGTTTA GTTTG
	M150V/M156V.R: CAAACTAAACACAGCTATT CTCATCTGCACTCCAATGTG ATGAAG
	M152V/M156V.F: CTTCATCACATTGGAATGCA GGTGAGAATAGCTGTGTTTA GTTTG
	M152V/M156V.R: CAAACTAAACACAGCTATT CTCACCTGCATTCCAATGTG ATGAAG
	M150V/M152V/M156V.F: CTTCATCACATTGGAGTGCA GGTGAGAATAGCTGTGTTTA GTTTG
	M150V/M152V/M156V.R: CAAACTAAACACAGCTATT CTCACCTGCACTCCAATGTG ATGAA G
pSP73 CFTR ex2-24	CFTRex3ATG/GTGDIR: CTTCGGCGATGTTTTTTCTGGAGATTTGTGTTCTATGGAATC
	CFTR ex3 ATG/GTGREV: GATTCCATAGAACACAAATCTCCAGAAAAAACATCG CCGAAG
	CFTRex4ATG/GTGDIR: CTTCATCACATTGGAGTGCAGATGAGAATAGCTATG
	CFTRex4ATG/GTGREV: CATAGCTATTCTCATCTGCACTC CAATGTGATGAAG
	CFTRex4ATG/GTG152DIR: TGGCCTTCATCACATTGGAATGCAGGTGAGAATAGCTATGTTTAGT
	CFTRex4ATG/GTG152REV: ACTAAACATAGCTATTCTCACCTGCATTCCAATGTGATGAAGGCCA
	CFTRex4ATG/GTG2xDIR: TGGCCTTCATCACATTGGAGTGCAGGTGAGAATAGCTATGTTTAGT
	CFTRex4 ATG/GTG2xREV: ACTAAA CATAGCTATTCTCACCTGCACTCCAATGTGATGAAGGCCA
	CFTRexATG/GTG3XDIR: TGGCCTTCATCACATTGGAGTGCAGGTGAGAATAGCTGTGTTTAGT
	CFTRex43ATG/GTG3XREV: ACTAAACACAGCTATTCTCACCTGCACTCCAATGTGATGAAGGCCA

Iodide efflux assay

For the functional assessment of CFTR (the c.120del23, F508del mutants and wt as a control) the CFTR-mediated iodide (I⁻) efflux was measured at room temperature, as previously [19] using an I⁻-selective electrode (ThermoElectron Corporation, Waltham, MA) and forskolin (10 μM), genistein (50 μM) as CFTR cAMP agonist and potentiator, respectively. Data are expressed as means ± SEM (standard error of the mean).

Statistical Analyses

Statistical analyses were performed using Student's t test, with a value of $p<0.05$ considered statistically significant.

In vitro transcription and translation

For *in vitro* transcription and translation, the TnT Coupled Reticulocyte Lysate System (Promega, Madison, WI, USA) was used with [³⁵S]methionine, according to the manufacturers' instructions. SDS-PAGE (3%/6%) separation of protein products was followed by autoradiography.

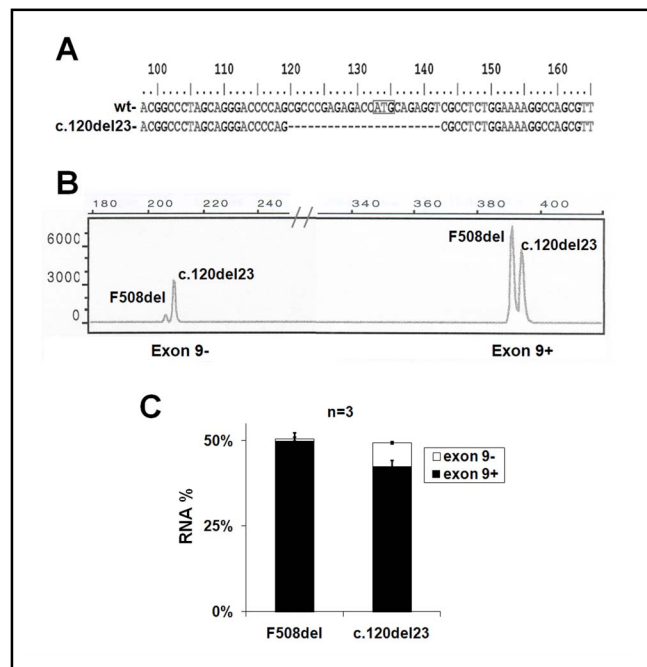## Results

CF Patients phenotype and DNA analysis

A Portuguese female patient from the Azores islands was diagnosed with CF at the age of 1 month by accepted criteria [20], including significant pulmonary involvement (bronchiectasis and bronchial obstruction), pancreatic insufficiency (PI) and elevated Cl⁻ in sweat (72 mmol/L, mean of two independent measurements); maxillary and ethmoid sinusitis; and suspicion of (but not confirmed) meconium ileus. As only one mutation (F508del) was identified by routine CFTR genotyping, we sequenced all CFTR exons and flanking intronic regions and found c.120del23 mutation (CFTR mRNA numbering as in GenBank:M28668). This mutation which had not been reported previously, except by ourselves [4] is localized in exon 1 and deletes 23 nucleotides (position 120 onwards) including the translation initiation codon (Fig.1A). This patient was previously analysed for the cAMP-mediated chloride (Cl⁻) secretion in the colon and no secretion was detected [21]. Subsequently, another unrelated Portuguese CF male patient, also with a severe clinical involvement (diagnosed at the age of 11 years; PI; 119 mEq/L Cl⁻ in sweat; mild bronchiectasis and lung colonization by *Pseudomonas aeruginosa*) was identified with the same genotype. To understand the disease-causing mechanisms of this novel mutation and to establish a correlation with the clinical phenotype, we studied its molecular, cellular and functional consequences.

Effect of the c.120del23 mutation at the RNA level

To evaluate whether c.120del23 alters the levels of CFTR transcripts, we quantified RNA from nasal epi-

Fig. 1. DNA and RNA analysis. (A) Alignment the wt-CFTR sequence (upper sequence) with the c.120del23-CFTR sequence (lower sequence) in the region of the mutation. The inset highlights the initiation translation codon M1 and the dashed line in the lower sequence corresponds to the nucleotides (23 nts) deleted by the mutation. (B) Representative analysis by capillary electrophoresis of RT-PCR products from transcripts of nasal epithelial cells from a CF patient with c.120del23/F508del genotype (see Methods), where the y-axis represents the fluorescence intensity and the x-axis the length of the RT-PCR products analysed (the // symbol represents a break in the scale). In the electropherogram the faster migrating products (appearing in the left) correspond to CFTR transcripts from both alleles lacking the exon 9, and the slower migrating products (in the right) correspond to the full-length transcripts (i.e., exon 9+). The areas beneath the peaks correspond to the amount of the PCR product amplified. (C) Graph summarizing quantification of transcripts (see Methods) shown in Fig1.B. Left - transcripts from the F508del allele; right - c.120del23 transcripts. In each column, the percentages of transcripts with and without exon 9 are represented as black and white areas, respectively. Graphs and error bars are mean ± standard deviation (SD) from independent RT-PCR assays (n=3).

thelial cells from one of the two above c.120del23/F508del patients. To this end, we applied a previously described quantitative (q) RT-PCR strategy (see Methods) which allows allele-specific quantification of CFTR transcripts when F508del is present in one allele and also enables quantification of exon 9 skipping [10]. The latter occurs to a lesser or greater extent depending on the intron 8 polymorphism $[TG]_m T_n$ [22]. This qRT-PCR approach enables detection of 4 different PCR products which in this patient are (Fig.1B): the two exon 9+ transcripts from c.120del23 (391 nt) and F508del (381 nt) alleles, both at the far right of the electropherogram; and the two exon 9- transcripts from c.120del23 (208 nt) and F508del (205 nt) alleles, at the far left. Fig.1C summarizes the quantification of these data (n =3) represented as the percentage of total CFTR transcripts from each allele (F508del, left; c.120del23, right) where values for exon 9+ and exon 9- transcripts are shown in black and in white, respectively. These results show that although levels of full-length (exon 9+) c.120del23 transcripts are lower than those from the F508del allele, this is because skipping of exon 9 (exon 9- transcripts) is higher for c.120del23- than for F508del-transcripts. However, this enhanced exon skipping in c.120del23 transcripts is plausibly not induced by the c.120del23 mutation *per se*, but rather by the $[TG]_{11} T_7$ polymorphism, which we found to be in *cis* with c.120del23 (data not shown), and which is described to cause more exon 9 skipping than the $[TG]_{10} T_9$ polymorphism which is in *cis* with F508del [22].

It should nevertheless be noted that the difference between the total levels of F508del and c.120del23-transcripts was not found to be statistically significant.

In silico analysis for putative in-frame alternative initiation codons

Next, we used "AUG evaluator" [10] to identify downstream AUG codons in CFTR mRNA (positions 1-4575 of GenBank:M28668) that could be used as alternative initiation codons according to the Kozak mRNA scanning model. This analysis revealed 82 AUGs of which only 38 are in-frame with M1 (Table 2). It also observed that all the out-of-frame AUGs identified would result in proteins smaller than in-frame CFTR (the largest having only 51 amino acids (aa)), due to the presence of premature termination codons (PTCs) (data not shown). The scores of the first four in-frame methionines downstream of M1 (M82, M150, M152 and M156) are shown in Table 2. Interestingly, all four have lower scores than M1, with the lowest (i.e, the methionine with the lowest probability of initiating CFTR translation) being M82 (exon 3). The scores of the other three methionines (M150, M152 and M156 all in exon 4) are very close to each other (Table 2) and truncated CFTR initiated at any of them would lack TM1 and TM2 (of MSD1), and the N-terminus. Sequence alignment of CFTR protein from several species [23] demonstrates that M1 and M150 are fully conserved through evolution and that M82 is the least conserved of the four

Ramalho/Lewandowska/Farinha/Mendes/Gonçalves/Barreto/Harris/Amaral

Table 2. *In silico* analysis of CFTR putative in-frame alternative initiation codons. Potential usage scores of the AUGs found in-frame with M1 in the CFTR mRNA (Genbank accession number M28668), as determined by the "AUG evaluator" software (see Methods). These scores correspond to a comparative sequence analysis of the consensus translation initiation site AUG and the sequence context of the AUGs found in-frame in the CFTR mRNA sequence. In *italic* (first row) is the AUG normally used *in vivo* to initiate CFTR translation (i.e., M1). The four AUGs immediately downstream of M1 (M82, M150, M152, M156) are in bold.

Position in mRNA	Position in protein	Sequence	Score	Protein lenght (aa)
133	*M1*	*CCGAGAGACC AUGCA*	*86.*	*1480*
376	**M82 (exon 3)**	**CUGGAGAUUU AUGUU**	**68.**	**1399**
580	**M150 (exon 4)**	**UCACAUUGGA AUGCA**	**76.**	**1331**
586	**M152 (exon 4)**	**UGGAAUGCAG AUGAG**	**74.**	**1329**
598	**M156 (exon 4)**	**GAGAAUAGCU AUGUU**	**75.**	**1325**
766	M212 (exon 6a)	GGCACUCCUC AUGGG	81.	1269
859	M243 (exon 6a)	GCUAGGGAGA AUGAU	81.	1238
862	M244 (exon 6a)	AGGGAGAAUG AUGAU	81.	1237
865	M245 (exon 6a)	GAGAAUGAUG AUGAA	80.	1236
925	M265 (exon 6b)	UACCUCAGAA AUGAU	79.	1216
973	M281 (exon 6b)	GGAAGAAGCA AUGGA	82.	1200
982	M284 (exon 6b)	AAUGGAAAAA AUGAU	78.	1197
1174	M348 (exon 7)	UGUUCUGCGC AUGGC	82.	1133
1312	M394 (exon 8)	AGAAGUAGUG AUGGA	82.	1087
1537	M469 (exon 10)	UUCACUUCUA AUGAU	72.	1012
1540	M470 (exon 10)	ACUUCUAAUG AUGAU	77.	1011
1546	M472 (exon 10)	AAUGAUGAUU AUGGG	77.	1009
1624	M498 (exon 10)	UUCCUGGAUU AUGCC	80.	983
1915	M598 (exon 13)	CUGUAAACUG AUGGC	77.	886
1951	M607 (exon 13)	CACUUCUAAA AUGGA	79.	874
2065	M645 (exon 13)	CUCAAAACUC AUGGG	74.	836
2293	M721 (exon 13)	UCCCUUACAA AUGAA	80.	760
2449	M773 (exon 13)	CCUGAACCUG AUGAC	78.	708
2641	M837 (exon 14a)	UUUUGAUGAU AUGGA	77.	644
2917	M929 (exon 15)	UUUGCUUGCU AUGGG	76.	552
2986	M952 (exon 15)	ACACCACAAA AUGUU	77.	529
3013	M961 (exon 15)	UCAAGCACCU AUGUC	79.	520
3214	M1028 (exon17a)	GGCUUUUAUU AUGUU	72.	453
3433	M1101 (exon 17b)	CUGGUUCCAA AUGAG	74.	380
3445	M1105 (exon 17b)	GAGAAUAGAA AUGAU	77.	376
3541	M1136 (exon 18)	GACUUUAGCC AUGAA	84.	344
3550	M1140 (exon 18)	CAUGAAUAUC AUGAG	77.	341
3601	M1157 (exon 19)	GGAUAGCUUG AUGCG	74.	324
3637	M1169 (exon 19)	GUUCAUUGAC AUGCC	79.	312
3703	M1191 (exon 19)	CUCGAAAGUU AUGAU	75.	290
3760	M1210 (exon 19)	AGGGGGCCAA AUGAC	84.	271
4192	M1354 (exon 22)	CAAGCAGUUG AUGUG	73.	127
4351	M1407 (exon 23)	GAUAGAAGCA AUGCU	79.	74

downstream methionines.

Effect of the CFTR c.120del23 mutation at the protein level

To determine whether c.120del23-CFTR mRNA uses any of these alternative codons *in vivo*, we produced a stable BHK cell line expressing the c.120del23-CFTR-cDNA-pNUT construct. Western blot analysis (Fig.2A) shows that this construct generates two CFTR-specific products (lane 2, Fig.2A, arrows D and E of ~133 and ~128 kDa, respectively), both of lower molecular mass than the immature ER form (known as band B ~140 kDa) of wt-CFTR (lane 1, Fig.2A). The slower migrating of these two forms (D) predomi-
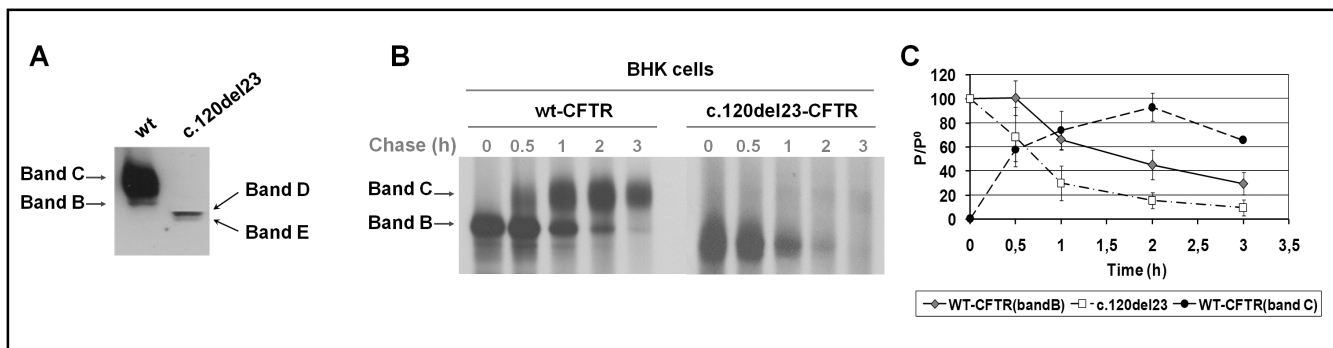
Fig. 2. Biochemical analyses of the c.120del23-CFTR variant. (A) Western blotting of total protein (30 μg) from BHK cells stably expressing wt- and c.120del23-CFTR. Lane 1, BHK cell line stably expressing wt-CFTR. Lane 2, BHK cell line stably expressing c.120del23-CFTR. D and E arrows indicate the positions of the upper and lower CFTR alternative translation initiation products. (B) Pulse-chase experiments followed by CFTR IP in BHK cells stably expressing wt- (left) or c.120del23-CFTR (right). The cells were pulse-labelled for 30 min with 100 μCi/ml [^{35}S]methionine and then chased for 0; 0.5; 1; 2; 3 h. (C) Graph showing the turnover of immature form (band B) of wt-CFTR (gray diamonds) and c.120del23-CFTR (open squares). The same graph also represents the efficiency of immature form (band B) processing into the mature form (band C) of wt-CFTR (black circles). Since the band C of c.120del23 protein (very faint) was only detected after 3 h of chase, it was not possible to quantify its efficiency of processing. Data correspond to the amount of labelled protein at chase time indicated as P relative to the amount of labelled protein at the start of the chase indicated as P^0. Symbols and error bars are means ± SD (standard deviation) of the values at each time point (n=3).

nates. Data in Fig.2A also indicate that expression levels of the mutant forms (lane 2) at steady-state are lower than those of wt-CFTR (lane 1). This quantitative difference is not the result of clonal variation in expression levels because lower expression levels were consistently observed for multiple c.120del23-CFTR clones in comparison to wt-CFTR clones (data not shown). These low levels may result from either decreased translation efficiency of the mutant protein, higher turnover or both.

To distinguish between these possibilities, we analysed the turnover rate of c.120del23-CFTR by pulse-chase experiments followed by IP (Fig.2B). The graph in Fig.2C shows that the turnover rate of immature c.120del23-CFTR is higher than that of immature wt-CFTR. Results in Fig.2B also show that c.120del23-CFTR is very inefficiently processed, as only a very faint band corresponding to its fully-glycosylated form is detected in comparison to that of wt-CFTR for which, after a 0.5h-chase, the fully-glycosylated form (band C) can already be observed. However, these data also suggest that a small fraction of the c.120del23-CFTR may traffic to the cell membrane.

Subcellular localization of c.120del23-CFTR and Cl$^-$ channel activity

To confirm that c.120del23-CFTR is present at the plasma membrane, we performed immunocytochemistry. Data in Fig.3, show that, whereas wt-CFTR is mostly

detected at the membrane, c.120del23-CFTR (Fig.3C) evidences a predominant intracellular staining, although with a more widespread distribution throughout the cytoplasm than F508del-CFTR (Fig.3B), but also with some faint staining appearing at the plasma membrane (arrows in Fig.3C). To further confirm the presence of c.120del23-CFTR at the cell membrane, we assessed its activity as a Cl$^-$ channel by the iodide efflux technique [24] which assesses the function of a population of CFTR Cl$^-$ channels in intact cells (see Methods). When cells expressing c.120del23-CFTR were treated with forskolin (FSK)/genistein (Gen), a detectable activity peak of iodide efflux was elicited (Fig. 4A, open squares) which is significantly lower (~25%, Fig.4B) than that of wt-CFTR (Fig. 4A black circles) but also significantly higher (~20%, Fig.4B) than that of F508del-CFTR (Fig.4A, grey triangles). Moreover, a delay of ~3 min in the peak response of 120del23-CFTR to agonists is also observed in comparison to wt-CFTR (Fig. 4A). Nevertheless, these data confirm that some c.120del23-CFTR is present at the cell membrane, albeit at very low levels.

Assessment of CFTR alternative initiation of translation

To determine which of the alternative AUG codons (Table 2) is used to initiate translation of the c.120del23-CFTR mRNA, resulting in the protein with the above-described properties, the four methionine
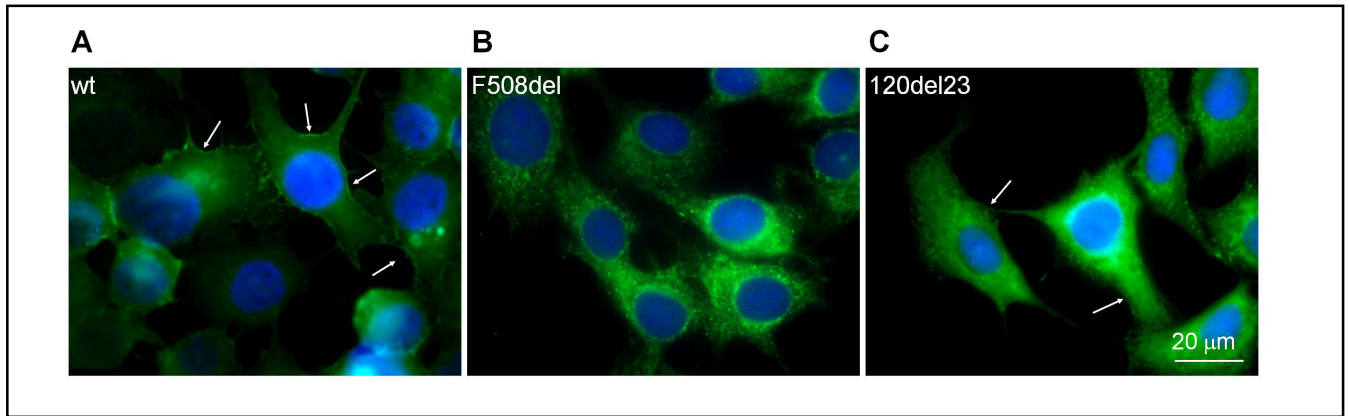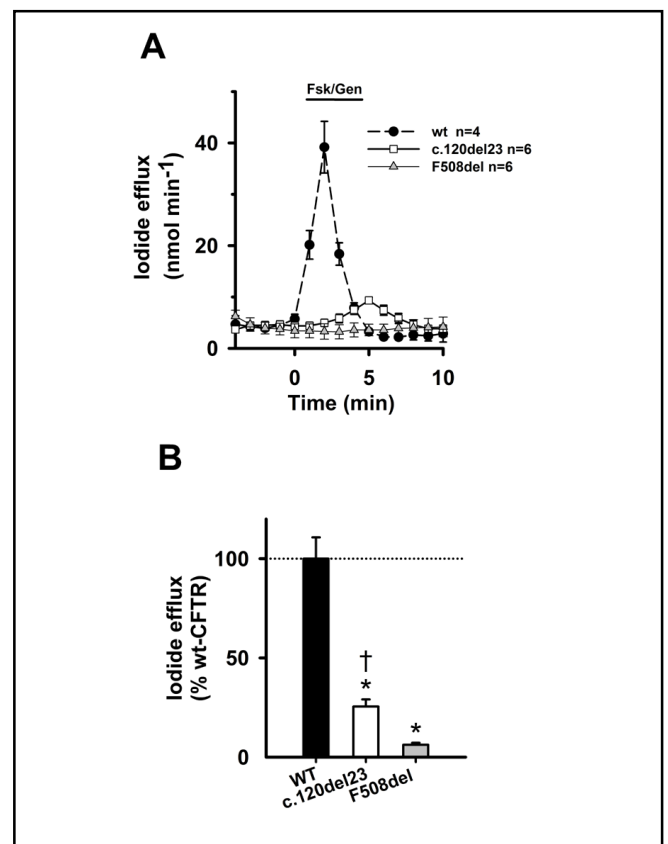
Ramalho/Lewandowska/Farinha/Mendes/Gonçalves/Barreto/Harris/Amaral

Fig. 3. CFTR protein resulting from the c.120del23 cDNA shows modest membrane localization. Immunocytochemistry analysis shows CFTR staining (green) at the membrane (see arrows) of wt-CFTR BHK cells (A), whereas in F508del-CFTR expressing cells (B) CFTR shows an intracellular staining pattern, consistent with the substantial ER-retention described for this mutant. In c.120del23-CFTR transfected cells (C), CFTR is detected predominantly intracellularly but some membrane staining is also observed (white arrows). For the nuclear staining we have used DAPI (blue). Data are representative of independent experiments (n=2) and no background staining or autofluorescence was observed with untransfected BHK cells. Bar = 20 μm.

Fig. 4. Functional assessment of c.120del23-CFTR by the iodide efflux assay shows partial function confirming membrane localization. (A) Time-course analysis of activity as a Cl⁻ channel and response to agonists (FSK/Gen) of c.120del23-CFTR expressed in comparison to wt and F508delCFTR (constructs stably expressed in BHK cells cultured at 37ºC) by the iodide efflux technique (see Methods). Black circles, open squares and gray triangles represent data from BHK-wt-CFTR, BHK-c.120del23-CFTR and BHK-F508del-CFTR cells, respectively. During the period indicated by the bar (in the upper part of the graph) forskolin (10 μM) and genistein (50 μM) were added to the efflux buffer. Abscissa: time, -4 to 10 min; ordinate: iodide efflux, 0 to 50 nmol min⁻¹. Symbols and error bars are mean ± SEM. Where not shown, errors bars are smaller than symbol size. (B) Summary of the peak iodide efflux magnitudes generated by c.120del23- and F508del-CFTR represented as a percentage of that of wt-CFTR. Asterisks and crosses represent significant differences from wt-CFTR and F508del, respectively $p < 0.05$. Data evidence a significantly decreased (~25%) and increased (~20%) global activity of the c.120del23-CFTR cells in comparison to wt-CFTR and F508del expressing cells, respectively.

codons (M82, M150, M152, M156) downstream of M1 (translation is a 5'->3' mechanism) were individually or jointly mutated into valines and the respective stable cells were analysed by immunoblot for CFTR. Results in Fig.5A reveal the presence of two proteins (D and E) for single mutants of M82V, M150V, M152V and M156V (lanes 3-6, respectively) and also for the double mutants M150V/M152, M150V/M156V and M152V/M156V (lanes 7-9). These two forms exhibit similar mobility to those detected for c.120del23-CFTR (lane 2). The upper of these (D
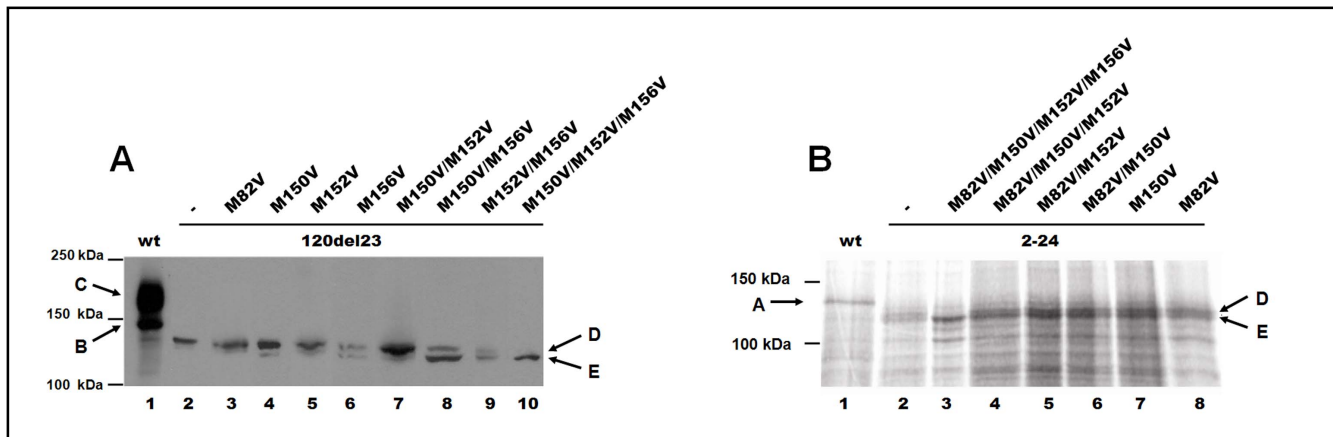
Fig. 5. Methionines in exon 4 of the CFTR gene all contribute to translation initiation in the absence of M1. (A) *In vivo* analysis. Total lysates of BHK cells stably transfected with the c.120del23-CFTR cDNA recombinant plasmids were analysed by immunoblot. The full length CFTR protein resulting from expression of wt- CFTR pNUT is observed in lane 1. Lane 2 – proteins resulting from expression of c.120del23-CFTR pNUT. Lanes 3-10 correspond to the proteins produced by the methionines mutants all in the c.120del23-CFTR pNUT background: lane 3, M82V; lane 4, M150V; lane 5 M152V; lane 6, M156V; lane 7, M150V/M152V; lane 8, M150V/M156V; lane 9, M152V/M156V; lane 10, M150V/M152V/M156V. Arrows D and E indicate the positions of the upper and lower CFTR protein products resulting from alternative translation, respectively. Data correspond to independent experiments (n=3). (B) Products of *in vitro* transcription/translation reactions separated on 3%/6% SDS/PAGE, gels dried and exposed to autoradiographic film. Lane 1, Full length wt-CFTR, plasmid pCMV936C. Lanes 2-8 all in pSP73: 2, CFTR exons 2-24; 3, M82V/M150V/M152V/M156V; 4, M82V/M150V/M152V; 5, M82/M152V; 6, M82V/M150V;7, M150; 8, M82V. Arrow A (on the left) indicates full-length translated wt-CFTR protein; D and E indicate the positions of the upper and lower alternative initiation products of ~133 kDa and ~128 kDa, respectively, which are predominantly observed for the CFTR mutants analysed here. Data correspond to independent experiments (n=3).

~133 kDa) is also observed when the wt-CFTR construct is analysed (lane 1) so CFTR alternative translation also occurs when M1 is present at the sequence. However, when the triple mutant (M150V/M152V/ M156V) was analysed (lane 10, Fig.5A), only the lower form (E ~128 kDa) could be detected. The failure to detect the larger form (arrow D) for this variant demonstrates that it corresponds to usage of M150, M152 or M156 (lane 10, Fig.5A). The shorter CFTR protein (arrow E) observed when the M150/M152 and M156 are simultaneously mutated probably results from usage of an AUG codon downstream of M156. In exon 6a four additional AUG codons (Table 2) are observed which can be used to initiate translation of this shorter CFTR version.

To confirm these data by *in vitro* translation (IVT), we used a cDNA construct lacking M1 (containing only CFTR exons 2-24) in the pSP73 vector and generated mutations in the same methionine residues. The cDNA CFTR exon 2-24 pSP73 construct mimics the alternative splicing CFTR transcripts lacking exon1 observed during the human and sheep lung development [25]. The IVT data shown in Fig.5B demonstrates that a number of smaller protein products were generated from the CFTR exon 2-24-pSP73 construct, including two prominent proteins (lane 2, arrows D and E), likely corresponding to the same species observed *in vivo*. The full-length immature form of wt-CFTR migrates at about 140 kDa (lane 1, arrow A, left). Additional products of CFTR exon 2-24-pSP73 construct IVT are observed (Fig.5B), likely resulting from usage of AUGs that are not used *in vivo* (Fig.5A) due to a more rigorous quality control of translation or from premature termination events. Individual and double mutations of M82V, M150V and M152V (lanes 5-8) did not cause loss of either protein species D or E, consistent with the corresponding constructs in the *in vivo* assay. The mutant M82V/M150V/M152V (lane 4) does not alter the production of proteins D and E either. However, the simultaneous deletion of all four methionines (M82, M150, M152 and M156) abolishes the production of the upper migrating protein at D (lane 3). Thus, this species likely corresponds to the CFTR variant resulting from usage of M150/M152 or M156 (and not of M82 because the M82V mutation alone did not abolish the appearance of this band).

Ramalho/Lewandowska/Farinha/Mendes/Gonçalves/Barreto/Harris/ Amaral

Discussion

Our aim here was to assess the functional impact at the molecular and cellular levels of the c.120del23 mutation, a novel mutation in the CFTR gene which we describe here for the first time in two Portuguese CF patients in compound heterozygosity with F508del.

The levels of c.120del23-mRNA are not decreased in native respiratory tissue

We first assessed the total levels of c.120del23 mRNA in native nasal cells from one of the above CF patients and found them to be at equivalent levels to F508del transcripts. This suggested that the mutation must generate CFTR protein(s), as translation usually precludes mRNA from degradation [26]. Moreover, our bioinformatic analysis indicates that all out-of-frame protein products (i.e., those resulting in open-reading-frames other than CFTR) bear premature stop codons (PTCs, data not shown). Hence, if these out-of-frame proteins were produced *in vivo*, significant degradation of the c.120del23-CFTR transcripts by nonsense-mediated mRNA decay (NMD) would be expected [27]. Our c.120del23 mRNA quantitative data thus predicts that out-of-frame proteins must not be produced at all *in vivo*.

Our data also reveal that higher levels of exon 9 skipping occur for c.120del23 transcripts than for F508del transcripts. However, these cannot be directly related to c.120del23 but rather to the $[TG]_{11}T_7$ polymorphism which in *cis* with the c.120del23-allele (not shown). Indeed, this polymorphism is known to induce higher levels of exon 9 skipping [22] than $[TG]_{10}T_9$ which is in *cis* with the F508del-allele.

The c.120del23 construct generates truncated forms of CFTR of reduced stability

To determine whether downstream in-frame AUG codons can be used to initiate CFTR translation in the absence of M1 in the c.120del23 construct, we performed WB analysis. Two CFTR alternative species (D and E, ~133 and ~128 kDa, respectively) with lower molecular mass than wt band B are detected, thus demonstrating usage of alternative initiation codons, consistently with previous studies with other CFTR variants [7]. These truncated forms of CFTR were consistently found at lower expression levels than wt-CFTR, possibly reflecting their lower efficacy in translation initiation [28], as predicted from the respective *in silico* efficacy scores.

An additional explanation for the low expression levels of c.120del23-CFTR at steady-state could be a faster degradation of the protein, as recently described for the Δ264 N-truncated CFTR [29]. Moreover, by WB only core-glycosylated forms of the c.120del23 were detected which also suggests low processing efficiency. Indeed, our results from metabolic pulse-labelling show that immature c.120del23-CFTR turns over faster than immature wt-CFTR (band B). This is an interesting finding since immature F508del-CFTR evidences no significant reduction in synthesis [30] or turnover [31, 32] relative to immature wt-CFTR. Since these experiments also show that maturation efficiency of c.120del23-CFTR is very low (mature c.120del23-CFTR form is very faint), the high turnover observed probably results from enhanced degradation, as indicated by previous studies [29, 33]. These reduced levels of processed c.120del23-CFTR can also result from reduced stability at the cell surface, as it was proposed that CFTR N-terminus plays a role in endocytosis through protein interactions, namely with cytoskeletal proteins [34, 35].

Altogether, these results for c.120del23-CFTR suggest an important role of the N-terminus in CFTR folding, stability and processing, which was also evidenced by other studies demonstrating that point mutations in this region - S50P; E60K; G85E/V; E92K - prevent CFTR maturation [35, 36]. Notwithstanding, since c.120del23-CFTR completely lacks the N-terminus it thus misses the arginine-framed-tripeptide (AFT) motif at residues 29-31 acting as a retention/retrieval signal for CFTR at the ER exit checkpoint [15]. The absence of this AFT would be predicted to enhance ER-to-Golgi transport of c.120del23-CFTR and this may actually account for the detection of the truncated protein at the plasma membrane.

Usage of CFTR alternative internal translation initiation codons

Next, we investigated which of the methionines with the highest probability of initiating translation (M82; M150; M152; and M156) originate the truncated forms CFTR of proteins detected here. Our *in vivo* and *in vitro* data indicate that M150, M152 and/or M156 may all be used to produce the major N-truncated CFTR protein (~133 kDa). It is not possible to determine which one is preferentially used, since in single-mutant experiments they appear as equivalent. In contrast, both *in vivo* and *in vitro* data demonstrate that M82 (the one with the lowest score and also the least conserved of the four), is not used to initiate CFTR translation. Since M150 has the highest score of the four and it is also the most conserved one, we predict that it is the codon which is selected *in*

vivo to initiate translation when M1 is missing (Fig.5A, lane 7 and 8). However, our data show that M152 and M156 can similarly be used to produce the form D (~133 kDa), at least when M150 is missing (Fig.5A lanes7-8). Although the most crucial nucleotides for AUG context are purine at -3 and guanine at +4 [28, 37], none of the CFTR AUG codons (including M1) analysed here has the latter. The fact that all three M150, M152 and M156 can be used to initiate alternative translation of CFTR, may result from a secondary structure on the mRNA at this region that enables the ribosome to recognize any one of them as initiation codon [38]. Indeed, these codons are used even in the presence of the M1 although at lower efficiency. Moreover, the fact that another truncated CFTR, of even greater mobility on SDS/PAGE (~128 kDa), is also produced when these three methionines are mutated, suggests the existence of another initiation codon further downstream of M156. Four additional AUG codons (in exon 6a) could initiate translation of this shorter CFTR protein, the first being M212. Other CFTR mutations reported in CF patients [4] that abolish M1 (M1V; M1K; M1T) will probably result in the production of the same N-truncated CFTR proteins as c.120del23 mutation. Moreover, it was previously showed that a transcript lacking exon 1, as a result of the recruitment of alternative 5' exons joined to exon 2, shows developmental regulation in the human and sheep lung [25]. This form also initiates at the methionines in exon 4 [39] suggesting a common function for this N-truncated protein.

Functional studies of 120del23-CFTR

Despite its intrinsic instability and the very low membrane levels of this mutant, we find here that c.120del23-CFTR, still has residual Cl- channel activity, in contrast to other CF-causing mutants like F508del-CFTR (this study) and R560T-, or A561E-CFTR [14, 15]. This may reflect a smaller impact on the CFTR Cl- channel activity by the most abundant N-terminal truncation product resulting from c.120del23-CFTR (i.e., M150/M152/M156 which remove TM1; TM2) in comparison to the above NBD1 mutations. Consistently, it was previously reported in *Xenopus* oocytes [7] that segments TM1-TM4 are not essential components of the

conduction pore or the selectivity filter of CFTR, although their removal causes lower conductance of the channel. However, in another study by Ge et al [40], segments M1 and M6 are defined as major contributors to the CFTR channel pore and Sheppard et al [41] demonstrated that the first half of CFTR forms a regulated Cl- channel with conduction properties similar to those of wt-CFTR.

Interestingly, recordings of c.120del23-CFTR by single-channel analysis were of two different types (André Schmidt and David Sheppard, personal communication), probably reflecting the presence of the two truncated CFTR forms detected here by Western blot (M150/M152/M156 and the shorter form). Both these types evidenced a detectable conductance, although of much lower open probability and burst durations than those of wt, consistent with the study by Carroll et al [7].

Overall, the biochemical data indicating that the prevalent N-truncated CFTR protein has decreased stability and very low processing efficiency together with these functional results showing that the c.120del23-CFTR has drastically reduced function, demonstrate a good correlation with the severe clinical CF phenotype of the two patients bearing this mutation. In previously analysis by Ussing chamber of native tissues from one of these patients, CFTR activity could not be detected [21]. This apparent discrepancy with our current results may simply derive from the higher CFTR expression levels in the systems employed here which allow enhanced sensitivity in functional measurements. Nevertheless, this study demonstrates the relevance of the molecular and functional characterization of mutations for the clinical setting.

Ramalho/Lewandowska/Farinha/Mendes/Gonçalves/Barreto/Harris/Amaral

References

1   Collins FS. Cystic fibrosis: molecular biology and therapeutic implications. Science 1992;256:774-9.

2   Gadsby DC, Vergani P, Csanady L. The ABC protein turned chloride channel whose failure causes cystic fibrosis. Nature 2006;440:477-83.

3   Riordan JR. CFTR function and prospects for therapy. Annu Rev Biochem 2008;77:701-26.

4   The CFTR mutation database. International Consortium for the Genetic Analysis of CF. http://www.genet.sickkids.on.ca/cftr/ . 2009.

5   Amaral MD. Processing of CFTR: Traversing the cellular maze-How much CFTR needs to go through to avoid cystic fibrosis? Pediatr Pulmonol 2005;39:479-91.

6   WHO CF report. The molecular Genetic Epidemiology of Cystic Fibrosis. 2004.

7   Carroll TP, Morales MM, Fulmer SB, Allen SS, Flotte TR, Cutting GR, Guggino WB. Alternate translation initiation codons can create functional forms of cystic fibrosis transmembrane conductance regulator. J Biol Chem 1995;270:11941-6.

8   http://central.igc.gulbenkian.pt/cftr/vr/f/ramalho_sequence_cftr_exons_clones_pac_library_rpcip704.pdf. 2009.

9   Ramalho AS, Beck S, Farinha CM, Clarke LA, Heda GD, Steiner B, Sanz J, Gallati S, Amaral MD, Harris A, Tzetis M. Methods for RNA extraction, cDNA preparation and analysis of CFTR transcripts. J Cyst Fibros 2004;3(S2):11-5.

10   Ramalho AS, Beck S, Meyer M, Penque D, Cutting GR, Amaral MD. Five percent of normal cystic fibrosis transmembrane conductance regulator mRNA ameliorates the severity of pulmonary disease in cystic fibrosis. Am J Respir Cell Mol Biol 2002;27:619-27.

11   AUG evaluator-http://l25.itba.mi.cnr.it/~webgene/wwwaug.html, Open Reading Frame Finder - http://www.ncbi.nlm.nih.gov/gorf/gorf.html. 2009.

12   Palmiter RD, Behringer RR, Quaife CJ, Maxwell F, Maxwell IH, Brinster RL. Cell lineage ablation in transgenic mice by cell-specific expression of a toxin gene. Cell 1987;50:435-43.

13   Tabcharani JA, Chang XB, Riordan JR, Hanrahan JW. Phosphorylation-regulated Cl- channel in CHO cells stably expressing the cystic fibrosis gene. Nature 1991;352:628-31.

14   Pissarra LS, Farinha CM, Xu Z, Schmidt A, Thibodeau PH, Cai Z, Thomas PJ, Sheppard DN, Amaral MD. Solubilizing mutations used to crystallize one CFTR domain attenuate the trafficking and channel defects caused by the major cystic fibrosis mutation. Chem Biol 2008;15:62-9.

15   Roxo-Rosa M, Xu Z, Schmidt A, Neto M, Cai Z, Soares CM, Sheppard DN, Amaral MD. Revertant mutants G550E and 4RK rescue cystic fibrosis mutants in the first nucleotide-binding domain of CFTR by different mechanisms. Proc Natl Acad Sci U S A 2006;103:17891-6.

16   Farinha C, Penque D, Roxo Rosa M, Lukacs GL, Dormer R, McPherson M, Pereira M, Bot AGM, Jorna H, Willemsen R, DeJonge R, Heda GD, Marino CR, Fanen P, Hinzpeter A, Lipecka J, Fritsch J, Gentzsch M, Jensen T, Aleksandrov A, Aleksandrov L, Riordan JR, Mengos A, Rhim AD, Stoykova LI, Trindade AJ, Glick MC, Scanlin T, Ollero M, Edelman A, Amaral MD. Biochemical methods to assess CFTR expression and membrane localization. J Cyst Fibros 2004;3(S2):73-77.

17   Farinha CM, Nogueira P, Mendes F, Penque D, Amaral MD. The human DnaJ homologue (Hdj)-1/heat-shock protein (Hsp) 40 co-chaperone is required for the in vivo stabilization of the cystic fibrosis transmembrane conductance regulator by Hsp70. Biochem J 2002;366:797-806.

18   Mendes F, Doucet L, Hinzpeter A, Ferec C, Lipecka J, Fritsch J, Edelman A, Jorna H, Willemsen R, Bot AG, de Jonge HR, Hinnrasky J, Castillon N, Taouil K, Puchelle E, Penque D, Amaral MD. Immunohistochemistry of CFTR in native tissues and primary epithelial cell cultures. J Cyst Fibros 2004;3(S2):37-41.

19   Schmidt A, Hughes LK, Cai Z, Mendes F, Li H, Sheppard DN, Amaral MD. Prolonged treatment of cells with genistein modulates the expression and function of the cystic fibrosis transmembrane conductance regulator. Br J Pharmacol 2008;153:1311-23.

20   Rosenstein BJ, Cutting GR. The diagnosis of cystic fibrosis: a consensus statement. Cystic Fibrosis Foundation Consensus Panel. J Pediatr 1998;132:589-95.

21   Hirtz S, Gonska T, Seydewitz HH, Thomas J, Greiner P, Kuehr J, Brandis M, Eichler I, Rocha H, Lopes AI, Barreto C, Ramalho A, Amaral MD, Kunzelmann K, Mall M. CFTR Cl- channel function in native human colon correlates with the genotype and phenotype in cystic fibrosis. Gastroenterology 2004;127:1085-95.

22   Cuppens H, Lin W, Jaspers M, Costes B, Teng H, Vankeerberghen A, Jorissen M, Droogmans G, Reynaert I, Goossens M, Nilius B, Cassiman JJ. Polyvariant mutant cystic fibrosis transmembrane conductance regulator genes. The polymorphic (Tg)m locus explains the partial penetrance of the T5 polymorphism as a disease mutation. J Clin Invest 1998;101:487-96.

23   Chen JM, Cutler C, Jacques C, Boeuf G, Denamur E, Lecointre G, Mercier B, Cramb G, Ferec C. A combined analysis of the cystic fibrosis transmembrane conductance regulator: implications for structure and disease models. Mol Biol Evol 2001;18:1771-88.

24   Norez C, Heda GD, Jensen T, Kogan I, Hughes LK, Auzanneau C, Derand R, Bulteau-Pignoux L, Li C, Ramjeesingh M, Li H, Sheppard DN, Bear CE, Riordan JR, Becq F. Determination of CFTR chloride channel activity and pharmacology using radiotracer flux methods. J Cyst Fibros 2004;3(S2):119-21.

25   Mouchel N, Broackes-Carter F, Harris A. Alternative 5' exons of the CFTR gene show developmental regulation. Hum Mol Genet 2003;12:759-69.

26   Shyu AB, Wilkinson MF, van Hoof A. Messenger RNA regulation: to translate or to degrade. EMBO J 2008;27:471-81.

27   Maquat LE. Nonsense-mediated mRNA decay: splicing, translation and mRNP dynamics. Nat Rev Mol Cell Biol 2004;5:89-99.

28   Kozak M. Pushing the limits of the scanning mechanism for initiation of translation. Gene 2002;299:1-34.

29   Cebotaru L, Vij N, Ciobanu I, Wright J, Flotte T, Guggino WB. Cystic fibrosis transmembrane regulator missing the first four transmembrane segments increases wild type and DeltaF508 processing. J Biol Chem 2008;283:21926-33.

30   Du K, Sharma M, Lukacs GL. The DeltaF508 cystic fibrosis mutation impairs domain-domain interactions and arrests post-translational folding of CFTR. Nat Struct Mol Biol 2005;12:17-25.

31   Lukacs GL, Mohamed A, Kartner N, Chang XB, Riordan JR, Grinstein S. Conformational maturation of CFTR but not its mutant counterpart (delta F508) occurs in the endoplasmic reticulum and requires ATP. EMBO J 1994;13:6076-86.

32 Ward CL, Kopito RR. Intracellular turnover of cystic fibrosis transmembrane conductance regulator. Inefficient processing and rapid degradation of wild-type and mutant proteins. J Biol Chem 1994;269:25710-8.

33 Lu Y, Xiong X, Helm A, Kimani K, Bragin A, Skach WR. Co- and posttranslational translocation mechanisms direct cystic fibrosis transmembrane conductance regulator N terminus transmembrane assembly. J Biol Chem 1998;273:568-76.

34 Jurkuvenaite A, Varga K, Nowotarski K, Kirk KL, Sorscher EJ, Li Y, Clancy JP, Bebok Z, Collawn JF. Mutations in the amino terminus of the cystic fibrosis transmembrane conductance regulator enhance endocytosis. J Biol Chem 2006;281:3329-34.

35 Thelin WR, Chen Y, Gentzsch M, Kreda SM, Sallee JL, Scarlett CO, Borchers CH, Jacobson K, Stutts MJ, Milgram SL. Direct interaction with filamins modulates the stability and plasma membrane expression of CFTR. J Clin Invest 2007;117:364-74.

36 Gene GG, Llobet A, Larriba S, de SD, Martinez I, Escalada A, Solsona C, Casals T, Aran JM. N-terminal CFTR missense variants severely affect the behavior of the CFTR chloride channel. Hum Mutat 2008;29:738-49.

37 Lukaszewicz M, Feuermann1 M, Jerouville B, Stas A, Boutry M. In vivo evaluation of the context sequence of the translation initiation codon in plants. Plant Sci 2000;154:89-98.

38 Kozak M. Influences of mRNA secondary structure on initiation by eukaryotic ribosomes. Proc Natl Acad Sci U S A 1986;83:2850-4.

39 Lewandowska M, Costa F, Bischof LM, Williams, SH, Soares MB, Harris A. Multiple mechanisms influence activation of the CFTR gene promoter. Am J Resp Cell Mol Biol. 2009. In press.

40 Ge N, Muise CN, Gong X, Linsdell P. Direct comparison of the functional roles played by different transmembrane regions in the cystic fibrosis transmembrane conductance regulator chloride channel pore. J Biol Chem 2004;279:55283-9.

41 Sheppard DN, Ostedgaard LS, Rich DP, Welsh MJ. The amino-terminal portion of CFTR forms a regulated Cl- channel. Cell 1994;76:1091-8.